Behavior of Cylindrical Steel Shells Supported on Local Brackets

Cornelia Doerich[1] and J. Michael Rotter[2]

Abstract: The connection of a local support to an elevated cylindrical metal silo shell is a long-standing difficult problem in shell analysis, and most designs are based on simple ideas using past experiences of successes and failures. Smaller silo structures are often supported on local brackets attached to the side of the shell, but very few investigations of the behavior or strength of such an arrangement have ever been made. This paper presents an outline description of the behavior of a cylindrical steel shell that is discretely supported on several brackets, each rigidly connected to a stiff column or floor. The linear, materially nonlinear, geometrically nonlinear, and bifurcation behaviors of the shell under these conditions are outlined. In this problem the prebuckling deformations, bifurcation mode, and plastic collapse mode are each local. This configuration presents some interesting questions concerning the relative importance of geometric nonlinearity and geometric imperfections. The problem is recommended to advanced shell analysts as a benchmark test of their analysis and interpretation techniques.

DOI: 10.1061/(ASCE)0733-9445(2008)134:8(1269)

CE Database subject headings: Shell structures; Supports; Silos; Tanks; Cylinders; Elastoplasticity; Collapse.

Introduction

For the storage of large quantities of particulate solids and fluids, a cylindrical shell metal structure with its axis vertical is usually the most economic. Metal silos and tanks are often required to be elevated above ground level to permit trains, trucks, or conveying systems to be placed beneath a hopper from which the solid or fluid is withdrawn. Elevated silos must be supported, and access requirements often mean that the supports must be local (either on columns or supported from an elevated floor system). The connection of such a support to a cylindrical shell is a long-standing difficult problem in shell analysis, and most designs use only past experiences of successes and failures. Smaller silo structures are often supported on local brackets attached to the side of the shell, but very few investigations of the behavior or strength of such an arrangement have ever been made.

Cylindrical shells with their axis vertical have long been supported at a few discrete locations around the axis (Fig. 1). In larger silos, the supports are usually placed beneath a ring beam at the transition [Fig. 1(d)], but in lighter structures, direct support of the shell on a number of brackets [Fig. 1(b)] or by engagement of a column into the shell wall is common [Fig. 1(c)]. These light support structures have often been designed by engineering judgment: there appear to be very few experiments that have explored their strength. With the increasing codification of consistent and comprehensive rules for design, the local support presents a significant challenge because the simpler analysis methods cannot be used to justify designs that have proved adequate in practice, but complex nonlinear calculations are usually out of the question in design evaluations of relatively inexpensive structures.

The stress analysis of a shell on discrete supports is a very challenging task. The first simple membrane theory calculations were probably performed in the 1930s by Flügge (1973), but the first linear shell analysis was that of Kildegaard (1969), which illustrated the complexity of the problem. This analysis covered only discrete point forces on the bottom boundary of the cylinder. Where the shell is supported on engaged columns, the problem of force transmission from an axially loaded strip into a plate is relevant, and the studies of Reissner (1940) and Gould et al. (1976) are particularly useful. A good review of early research on discretely supported cylinders was presented by Wang and Gould (1974). The present study is concerned with local bracket supports which were not previously considered. The most relevant earlier work was that of Bijlaard (1955), who devised a linear analysis of the stresses resulting from a local patch load normal to the shell. The equivalent analyses for an axially loaded patch were presented by Li and Rotter (1996).

Peter (1974) made the first linear buckling analysis, again for point forces beneath the shell, but nonlinear analyses were not possible until high powered computational tools were available. More recent computational studies by Teng and Rotter (1990, 1992), Rotter et al. (1991), Guggenberger (1991, 1998), Greiner and Guggenberger (1998), and Guggenberger et al. (2000) have only addressed local forces applied to the base boundary of a cylindrical shell.

The bracket supported shell is more widely used where the silo is within a building (Fig. 2). The only known strength evaluations of this arrangement (Gillie et al. 2002; Holst et al. 2002) involved brackets that were free to rotate about a circumferential axis [Fig. 2(b)], which corresponds to a weaker and less likely condition

[1]Dr., Institute for Infrastructure & Environment, Univ. of Edinburgh, Mayfield Rd., Edinburgh, EH9 3JL, U.K.

[2]Professor, Institute for Infrastructure & Environment, Univ. of Edinburgh, Edinburgh EH9 3JL, U.K. (corresponding author). E-mail: m.rotter@ed.ac.uk

Note. Associate Editor: Benjamin W. Schafer. Discussion open until January 1, 2009. Separate discussions must be submitted for individual papers. To extend the closing date by one month, a written request must be filed with the ASCE Managing Editor. The manuscript for this paper was submitted for review and possible publication on April 2, 2007; approved on January 28, 2008. This paper is part of the ***Journal of Structural Engineering***, Vol. 134, No. 8, August 1, 2008. ©ASCE, ISSN 0733-9445/2008/8-1269–1277/$25.00.

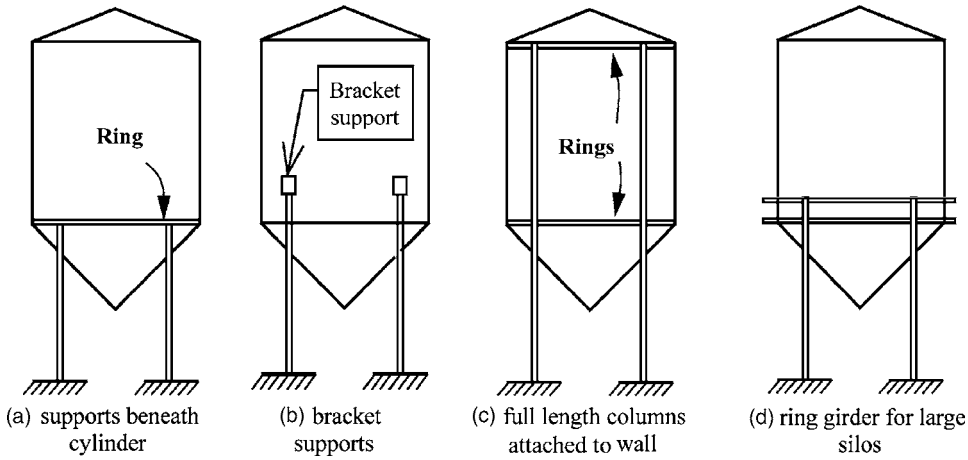

Fig. 1. Alternative arrangements for silos on discrete supports

than is typically found in practice. The present study involves an extensive exploration of the elastic-plastic strength of an imperfect cylindrical shell attached to a bracket that is restrained by the column or support against rotation [Fig. 2(c)], producing a much stronger detail.

United States standards for the design of shell structures are principally oriented towards aerospace applications (Nemeth and Starnes 1998) and unfortunately are not yet sufficiently developed to address the interpretation of advanced finite-element analyses for local support problems. The study has therefore been conducted within the framework of the European Standard for Shell Structures (CEN 2006), which requires that the two reference strengths of the shell, the plastic collapse resistance, and the linear bifurcation resistance, should both be evaluated to establish the context within which more sophisticated analyses are judged, and to provide a rapid means of producing reliable but simple design information.

Modeling of Bracket and Shell

The shell had radius r, uniform thickness t, and height H. The bracket was located at the height ηH above the base of the shell, and had height h and width $2d$ [this notation was adopted to be compatible with that used for supports at the shell base by Guggenberger et al. (2000)]. The bracket was treated as extremely stiff, to eliminate this aspect from the study. A notional ratio of bracket to shell thickness of $t_b/t=200$ was adopted, rigidly attached to the shell wall, as shown in Fig. 3(a). Explorations of the effect of this thickness indicated that this was sufficient to model a completely stiff bracket (Doerich 2007). The full cylinder was loaded by a meridional tension P per unit circumference at the lower edge [Fig. 3(b)], corresponding to the loading applied by contained fluid or solid via a hopper beneath the cylinder.

The shell was treated as ideally elastic-plastic with Young's modulus E, Poisson's ratio ν, and yield stress σ_Y with von Mises yield criterion. It is recognized that strain hardening will affect the strength under highly plastified conditions, but hardening was omitted from the present study for the sake of clarity and simplicity. It will be included in future studies. In these calculations, a cylinder with four bracket supports ($n=4$) was studied because this is the most common arrangement in practice.

The problem was studied using the commercial finite-element (FE) package ABAQUS (HKS 2003). The analysis used two element types, both of which are rectangular doubly curved shell elements with reduced integration and hourglass control. Most of the model used the four-noded general-purpose S4R element, but in the zone around the bracket the eight-noded thick shell element S8R was used because of its superior performance in highly plastified zones. To reduce the size of the computations, symmetry was exploited down the meridian through the center of the bracket, as well as down the midplane between brackets, reducing the model to one eighth of the complete shell, though sample results were verified by comparison with a full model of the entire shell. The bracket was treated as free to translate radially, but all other degrees of freedom were deemed to be restrained by the stiff column. At the top and bottom edges, no out-of-round deformation was permitted, simulating stiff rings.

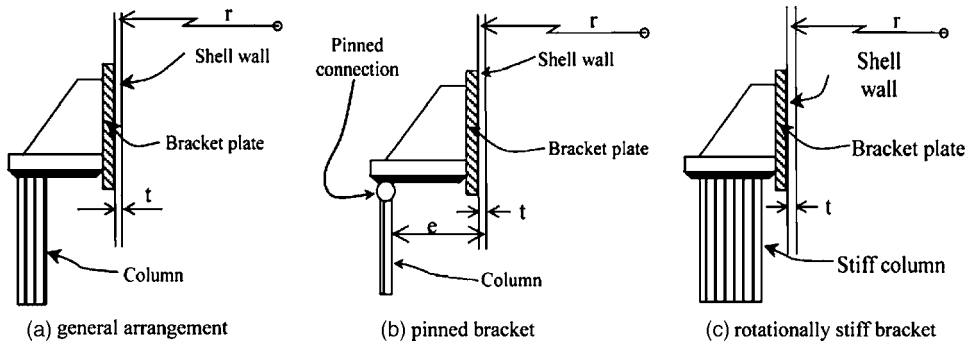

Fig. 2. Alternative treatments of bracket support

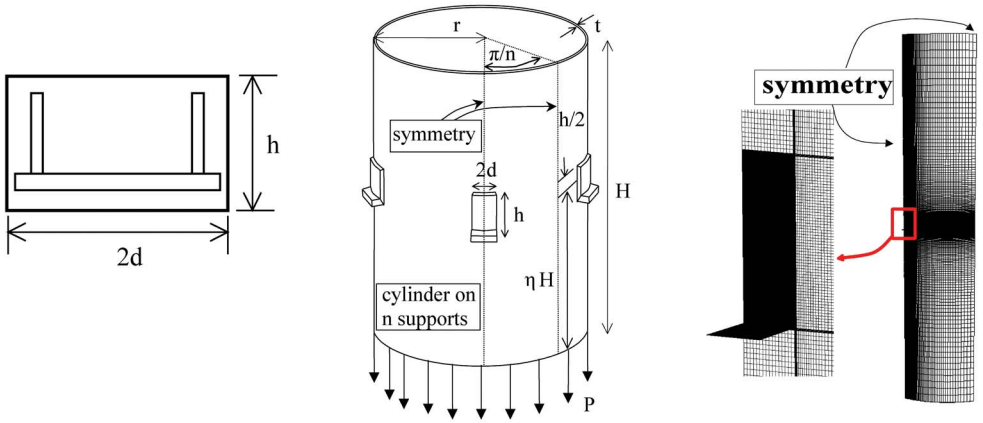

Fig. 3. Dimensions and finite-element model

The mesh was verified extensively (Doerich 2007) using the linear analysis (LA), elastic geometrically nonlinear analysis (GNA), small displacement theory elastic-plastic analysis (MNA), and geometrically nonlinear elastic-plastic analysis (GMNA) defined in EN1993-1-6 (CEN 2006). Particular attention was paid to the region of the corner of the bracket where a high stress concentration occurs (Doerich 2007). These analyses were also widely checked against those of Gillie (2002) for unrestrained brackets. The finite-element mesh used, resulting from this mesh verification process, is shown in Fig. 3(c). Where geometric nonlinearity was used, the analysis included the effects of large rotations, but not large strains.

Example Bracket Support

An example bracket support is studied here to explore the characteristics of the behavior. This bracket was chosen to have a geometry in which there is significant interaction between elastic buckling and plasticity, even though the shell is thin, placing it clearly in the elastic-plastic buckling regime for this structure. The manner in which this choice was made is shown later.

The key parameters of this representative problem were: $H/r=4$, $r/t=600$, $\eta=0.5$, $h/r=0.12$, $h/d=3$, and $n=4$, with $E=2\times10^5$ MPa, $\nu=0.3$, and $\sigma_Y=250$ MPa. In the following analyses, all the loads are described in a dimensionless manner, using the reference force R_{REF} applied to each bracket:

$$R_{REF}=\sigma_{cl}(A/n)=\sigma_{cl}(2\pi rt/n) \quad (1)$$

in which the classical elastic critical buckling stress σ_{cl} for uniform axial compression is given by

$$\sigma_{cl}=0.605Et/r \quad (2)$$

The force R_{REF} is used to normalize all the strength calculations. This reference load corresponds to the classical elastic critical stress for uniform axial compression being applied in tension around the full shell circumference at its lower edge.

In the following, the results of the different analyses defined by in EN1993-1-6 (CEN 2006) are shown. These begin with the reference analyses of LA, linear bifurcation analysis (LBA), and plastic reference load (MNA), and are followed by GNA and GMNA, and analyses including explicitly modeled imperfections (GMNIA). The role of each of these different analyses was described by Rotter (1998).

Linear Elastic Analysis

The simplest treatment of this problem is a linear elastic analysis. It is useful to study the pattern of load transfer from the tension near the shell base into the bracket, in preparation for an understanding of the behavior found later in other analyses. In simple terms, one might expect that the vertical tension from the load on the base circumference [Fig. 3(b)] would be fed into the base of the bracket, perhaps with some shear transfer onto the side of the bracket. The first images worthy of study are therefore the axial membrane stress pattern and the membrane shear pattern in the shell.

The bracket causes an inward deformation of the shell for a significant height above it, leading to inward bending in both the circumferential and meridional directions [Fig. 4(a)]. Further, the wall becomes flatter in this region, which is later seen to have a detrimental effect on the buckling strength. Fig. 5(a) shows the axial membrane stress on horizontal lines at several different levels in the shell. At the bottom, the load is applied and there is the

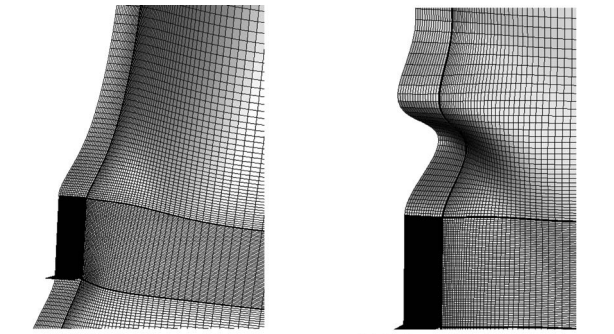

Fig. 4. Linear elastic deformations (LA) and linear bifurcation mode (LBA)

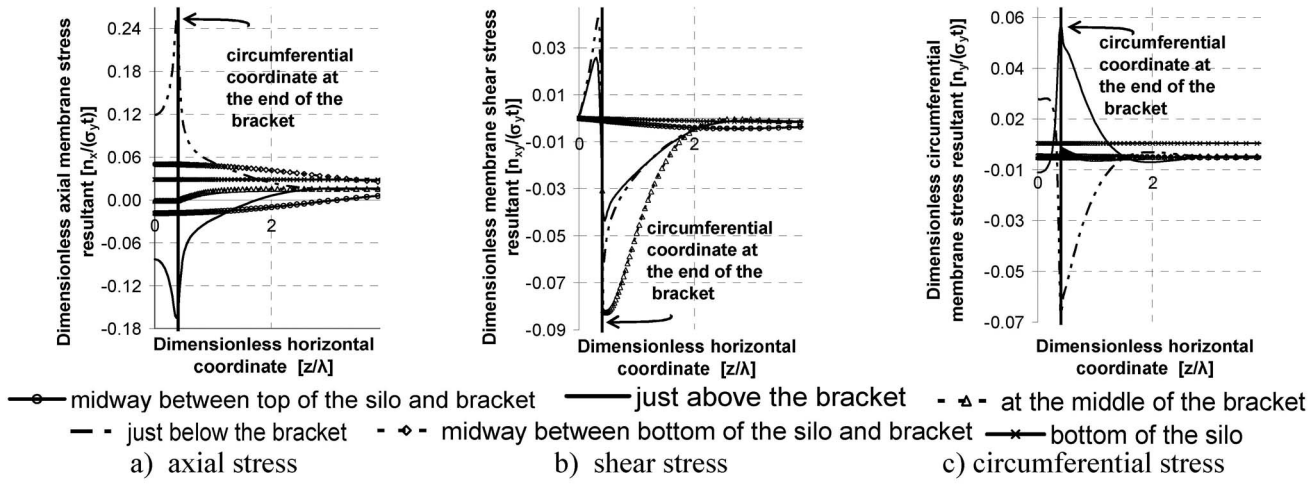

Fig. 5. Dimensionless stress resultants at different heights in silo (LA)

expected uniform axial tension. Half way between the base and the bracket, elevated tensile stresses develop towards the bracket meridian, with a corresponding decrease away from the bracket meridian. Just below the bracket, high tensile stresses focus into the bracket, with a distribution similar to that of a rigid footing on an elastic half space (Timoshenko and Goodier 1970). Extensive studies were undertaken of mesh sensitivity in this region, particularly for the nonlinear analyses reported later (Doerich 2007).

A strong peak can be seen at the bracket corner, but tensile stresses also continue in the shell away from the bracket meridian, ensuring that most of the load (in this example 70%) bypasses the bracket to induce shear and compression in the shell above it. In this example, 47% of the load is transferred in shear into the side of the bracket [Fig. 5(b)] with a peak in membrane shear at mid-height of the bracket. Above the bracket, load (here 23%) is transferred by compression into the top of the bracket [Fig. 5(a)], with a similar high peak to that below the bracket associated with the bracket corner. It is clear that the corners of the bracket represent points of strong stress concentration, and that local plasticity will affect the behavior here quite strongly, augmented by strain hardening. These are also points at which high shell bending stresses develop.

The circumferential membrane stresses are shown in Fig. 5(c), where it can be seen that high circumferential membrane stresses are developed near the top and bottom of the bracket through Poisson effects which arise due to the restraint of displacements by the stiff bracket. Thus this is another case where high stiffness leads to unexpected stresses and here they affect the first yield condition strongly (tensile where the axial stress is compressive, and vice versa).

Estimating Plastic Strength of Shell from Linear Analysis

It is not a simple task to determine the potential failure state of a shell from a linear elastic analysis. The first type of failure that might be considered here would be a yielding failure, which should strictly involve a fully developed plastic strain velocity field involving both bending and stretching of the shell (Massonnet and Save 1972). But since such an analysis is very onerous to perform, whether by hand or computationally, it is not reasonable to expect that all analysts will use a small displacement theory MNA of the structure to obtain the plastic collapse load. Consequently, the European shell standard EN1993-1-6 defines how this load can be estimated from the results of a linear elastic analysis. Since such an estimate is not easy to make, several alternative criteria were applied in the present study to see how effective they might be. The three criteria chosen for this investigation were: (1) first surface yield; (2) first surface yield according to the Ilyushin yield criterion, which is recommended in EN1993-1-6 (CEN 2006); and (3) first membrane stress resultant yield. All three estimates used the von Mises criterion to combine the stress components.

These three estimates of the plastic collapse strength were compared with the formal limit load calculated using ABAQUS, which is described below. The results show that all three criteria lead to very conservative estimates of the collapse strength. The first surface yield criterion predicts failure at 14.8%, the Ilyushin criterion predicts failure at 12.4%, and first membrane yield at 20.8% of the true plastic collapse load. These conservative predictions are caused by the high stress concentration at the corners of the bracket. Clearly more research is needed to find better criteria to use in estimating the plastic collapse strength from the results of a linear analysis.

Linear Bifurcation Analysis

Following a linear elastic analysis, it is a simple matter to determine the linear bifurcation load computationally. The lowest linear elastic bifurcation mode for the example bracket is shown in Fig. 4(b). This mode is quite local and lies just above the bracket. The first 17 eigenmodes were calculated, but only the first two were closely spaced (difference 4%), and these had very similar forms. The LBA buckling load R_{LBA} for this geometry is found to be $R_{\mathrm{LBA}}/R_{\mathrm{REF}}=0.450$ even though this load is applied as a tensile force at the bottom of the shell. If it is assumed that the support force is taken only in compression above the bracket and this result is reinterpreted in terms of the mean compressive stress just above the bracket σ_{ub}, it is found that $\sigma_{\mathrm{ub}}/\sigma_{\mathrm{cl}}=9.09$, so that even if the compression is deemed to be only one third of the total load transmission, the mean vertical stress above the bracket is a poor estimate of this simplest of all buckling strength estimates.

Geometrically Nonlinear Analysis

When a GNA is used for the prebuckling calculation, the prebuckling path is close to linear and the buckling load

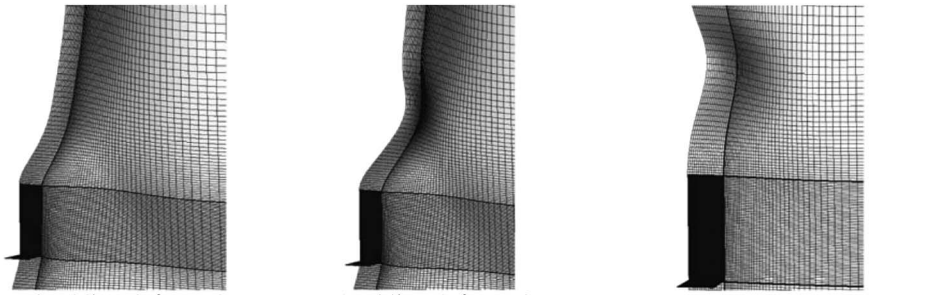

Fig. 6. Deformation just before and just after buckling in geometrically nonlinear elastic analysis and resulting incremental buckling mode

($R_{GNA}/R_{REF}=0.297$) is found to be much lower than the bifurcation load of an LBA analysis. The strength reduction due to geometric nonlinearity is 36%. This shows that the local bending deformations of the prebuckling state modify the buckling resistance of the shell considerably, as was seen also in the calculations for other local stress conditions by Holst and Rotter (2004) and Cai et al. (2002). It may be noted that in uniformly compressed cylinders, geometric nonlinearity leads to a strength reduction of typically 15% (Yamaki 1984), so this 36% reduction shows that geometric nonlinearity is very important here. Where local bending phenomena occur in a zone where a local buckle may form, the effects of geometric nonlinearity are usually very much greater than under conditions of uniform loading.

The prebuckling shape just before and the postbuckling deformed shape just after the peak load are shown in Fig. 6. The prebuckling deformations extend far above the bracket and the postbuckling deformed shape naturally includes these deformations. The incremental change between these two forms was therefore evaluated to extract the nonlinear incremental buckling mode [Fig. 6(c)]. The shape and location of the elastic nonlinear buckle is significantly different from the linear bifurcation mode [Fig. 4(b)]. The prebuckling deformed shape [Fig. 6(a)] shows an enlarged flattened zone above the bracket, which leads to lower curvature and is principally responsible for the reduction in buckling strength.

The elastic geometrically nonlinear load-deflection curve is shown in Fig. 7 (dotted), where the nonlinear bifurcation event can be seen to cause a sudden decrease in load, as is typical in compressed shells. The membrane stress patterns seen in this analysis are shown in Fig. 8. Three different points on the load deflection curve have been taken: one well before buckling in the elastic range, one just after buckling, and one at the lowest load on the postbuckling path. The axial membrane stress resultant [Fig. 8(a)] shows that the compressive peak near the corner of the bracket is increased after buckling, as might be expected since the buckle softens the zone above the middle of the bracket. In this middle zone, the compression is highest just after buckling, but it decreases rapidly near the postbuckling minimum and moves to be tensile deep in the postbuckling range.

The circumferential membrane stress resultant above the bracket [Fig. 8(b)] is dominated by a high tension developing at the bracket corner, exacerbating the high local axial compression in this location and causing early yield. These stresses are sustained after buckling, making this high stress concentration susceptible to yield despite the changes in geometry elsewhere caused by buckling. The membrane shear stresses at the midheight of the bracket [Fig. 8(c)] and the circumferential membrane stresses below it [Fig. 8(d)] are substantially unchanged by the buckling event. However, deep in the postbuckling regime, high circumferential tensile stresses develop over the bracket top.

Materially Nonlinear Analysis

When ideal elastic-plastic material nonlinearity is introduced, but small displacement theory is still adopted (no change in geometry), the calculation leads to the reference MNA plastic collapse load ($R_{MNA}/R_{REF}=0.257$). The form of the load-deflection curve is classic [Fig. 7 (black squares)], with significant plastic deformations developing at loads well below the collapse load, but with a horizontal plateau at the collapse load. The collapse load corresponds very well to a simple theoretical calculation of full plasticity around the bracket $R_{Ref}=2\cdot 2d\cdot t\cdot 2/\sqrt{3}\cdot\sigma_y + 2\cdot h\cdot t\cdot\sigma_y/\sqrt{3}$ (Fig. 9), fully exploiting the biaxial stress state provided by the restraint of the bracket. This bracket geometry was specially selected to be in the range where strong interactions are expected between plasticity and stability, so the MNA plastic collapse load is similar to the elastic nonlinear buckling load (Fig. 7). The membrane stress patterns in the plastic collapse mechanism and at different heights in the silo are shown in Fig. 10. The axial membrane stress resultant [Fig. 10(a)] reaches the limits of the von Mises envelope $\pm(2/\sqrt{3})\sigma_Y \approx \pm 1.155\sigma_Y$ [Fig. 9(a)], above and below the bracket, but away from the bracket it decreases to the applied load per unit circumference. The circumferential membrane stress resultant [Fig. 10(b)] immediately above and below the bracket reaches the corresponding reaction stress $\pm\sigma_Y/\sqrt{3} \approx \pm 0.577\sigma_Y$, again consistent with this point on von Mises ellipse, but away from the bracket it decreases to zero.

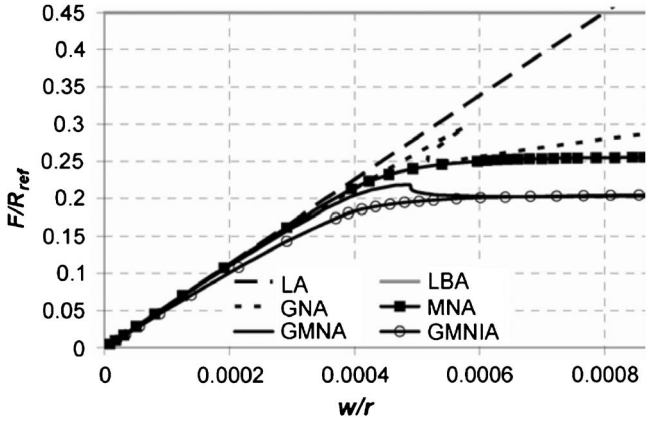

Fig. 7. Load-displacement curves for different analysis types

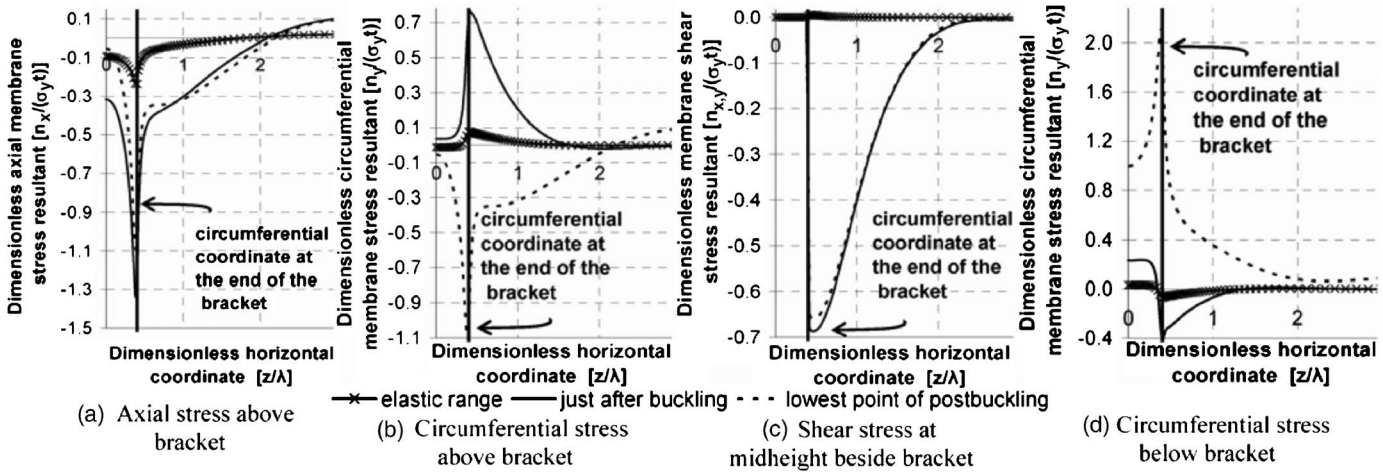

Fig. 8. Dimensionless membrane stress resultants at different loading stages (GNA)

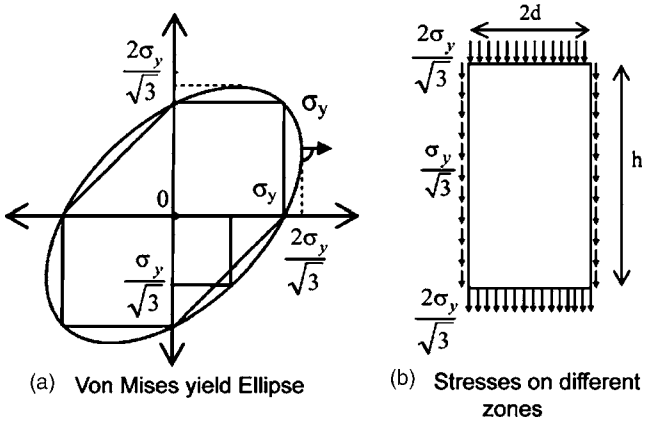

Fig. 9. Simple membrane stress calculation of plastic collapse strength

Under fully plastic conditions, the stresses above and below the bracket are symmetrical (Fig. 10), though under elastic conditions the axial tension below the bracket was, of course, dominant.

Geometrically and Materially Nonlinear Analysis (GMNA)

When both geometrical and material nonlinearities are included (GMNA), the limit load or bifurcation seen in the geometrically nonlinear elastic analysis is, perhaps naturally, removed (Fig. 7) and the shell moves smoothly from an unsymmetrical prebuckling deformation pattern into a different unsymmetrical postbuckling form, passing through a limit load ($R_{GMNA}/R_{REF}=0.219$) as it does so. For this geometry, this limit load is slightly below the plastic collapse (MNA) and nonlinear elastic bifurcation (GNA) loads.

The patterns of von Mises equivalent stress on the outer surface of the silo are shown in Fig. 11. In the elastic range [Fig. 11(a)], the maximum surface equivalent stress lies beneath the corner of the bracket. Just before buckling [Fig. 11(b)] yield has occurred around most of the bracket, and just after buckling [Fig.

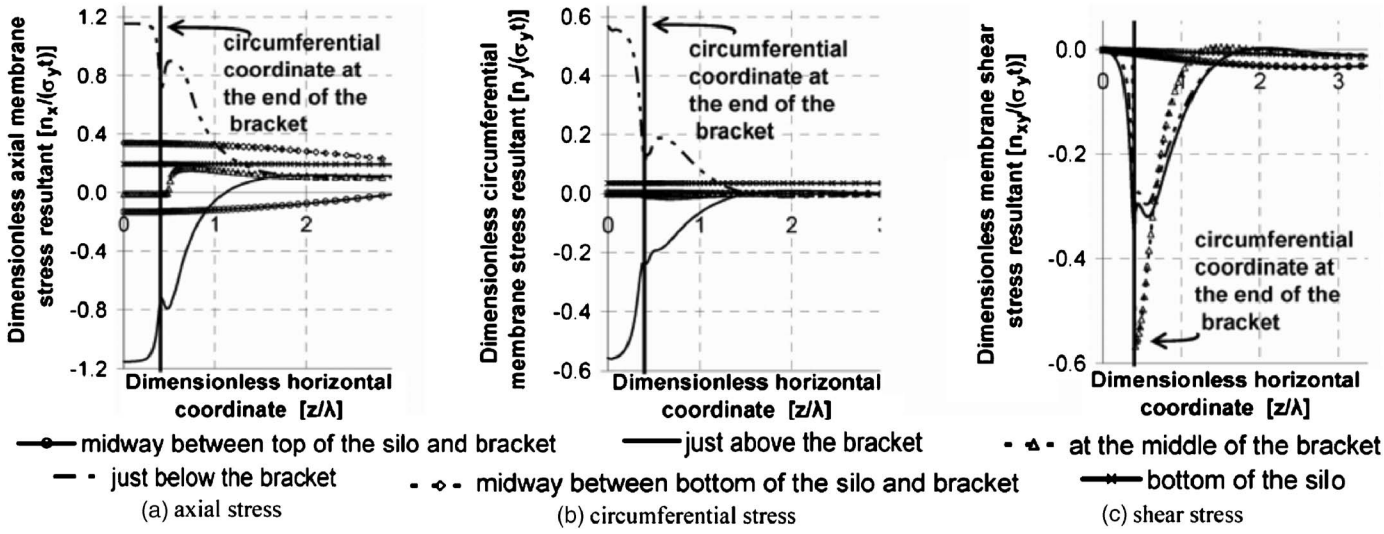

Fig. 10. Dimensionless membrane stress resultants at plastic collapse

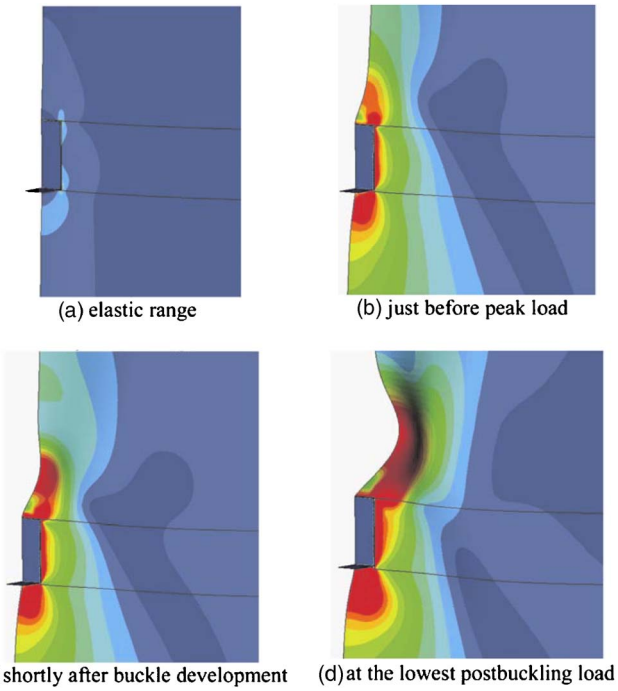

Fig. 11. von Mises stress distribution on outer surface (GMNA analysis: deformation factor 15)

11(c)] the local inward directed buckle above the bracket has caused an extension of the yield zone. At the lowest load on the postbuckling path [Fig. 11(d)], this deepening local buckle becomes extensively yielded. The images in Fig. 11 were taken from the ABAQUS (HKS 2003) postprocessor.

The distributions of the membrane stress resultants in the geometrically and materially nonlinear analysis are shown in Fig. 12 on three horizontal lines adjacent to the bracket. The stress states at three different points on the load deflection path (Fig. 7) are shown: one in the elastic range, one just after bucking, and one far into the postbuckling range. The sharp stress concentration in axial membrane stress seen in the elastic range at the bracket corner [Fig. 8(a)] is rapidly smoothed by yielding after buckling [Fig. 12(a)] and a rather uniform stress transfer develops at the peak attainable stress of $(2/\sqrt{3})\sigma_Y \approx 1.155\sigma_Y$ and this is sustained deep into the postbuckling range. The axial membrane stress resultant above the bracket shows a different behavior: the elastic peak compression that developed at the corner [Fig. 5(a)] moves inwards to be over the bracket after buckling, but is accompanied by a big drop in compression just beyond the corner. This drop is exacerbated in the postbuckling range. However because these stresses are strongly affected by the presence of the buckle, the uniform stress state seen in an MNA analysis [Fig. 10(a)] does not develop. The circumferential membrane stress resultant [Fig. 12(c)] sustains the same peak at the corner throughout, but in the postbuckling range it falls to zero above the bracket. These differences between geometrically nonlinear and materially nonlinear stress patterns illustrate the strong interactions between changes of geometry and stress smoothing due to plasticity.

The dimensionless membrane shear resultant on a horizontal line through the middle of the bracket [Fig. 12(d)] sustains the same form from prebuckling, through buckling, and into the postbuckling range, only limited by the von Mises limit in shear $\sigma_Y/\sqrt{3} \approx 0.577\sigma_Y$ and is unaffected by the buckle above the bracket. There is no suggestion of a plastic shear buckle here, even after extensive deformation, chiefly because the shear stress drops very quickly away from the bracket and there is not a large enough highly stressed zone for a buckle to develop. This is a common phenomenon in zones where shear stresses are locally high. It may be noted that a point-by-point assessment of the buckling strength, as prescribed in design standards (DASt-Richtlinie 1980; CEN 2006), is therefore very conservative if it depends on a high shear component.

In conclusion, the cylinder yields in shear on the side of the bracket just after buckling and in tension in the postbuckling range just below the bracket.

Geometrically and Materially Nonlinear with Explicit Imperfections Analysis

Many, but not all, shell buckling configurations show considerable sensitivity to geometric imperfections. It is therefore most important to establish how imperfection sensitive the bracket-supported cylinder might be. The effect of a geometric imperfection was explored using a materially and geometrically nonlinear analysis with imperfections explicitly defined (GMNIA), and introducing a linear eigenmode imperfection [Fig. 4(b)], as pro-

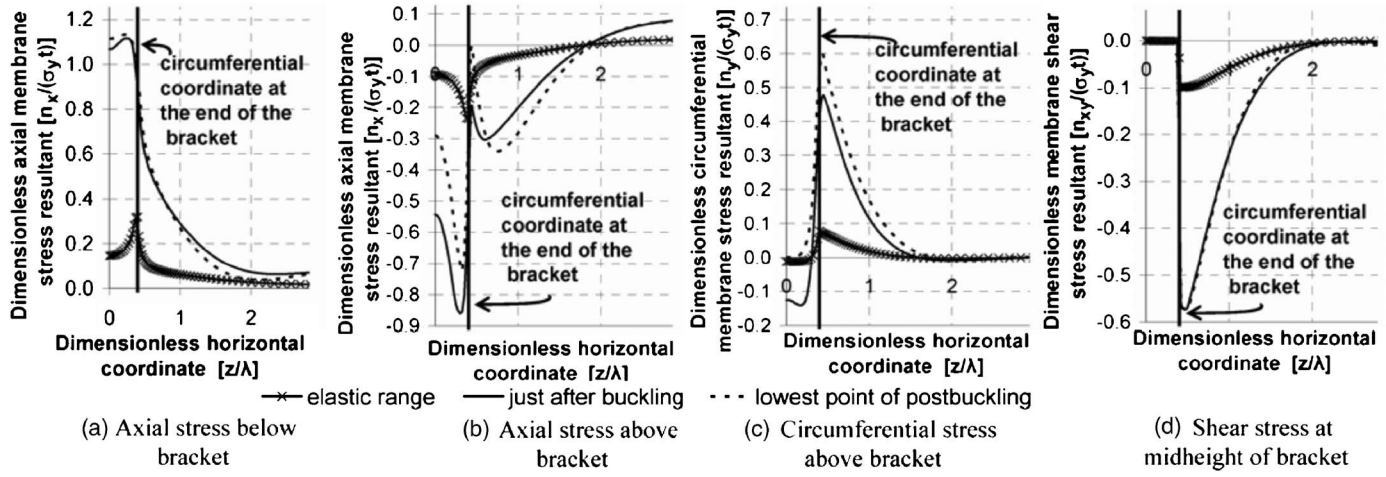

Fig. 12. Dimensionless membrane stress resultants at different load stages (GMNA)

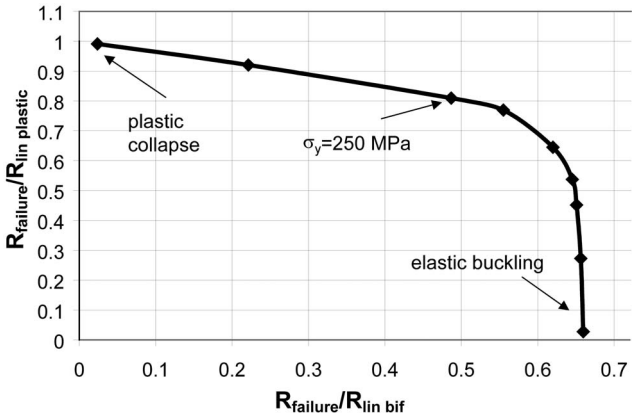

Fig. 13. Capacity curve for shells of different slenderness

posed in EN1993-1-6 (CEN 2006), with an amplitude of one wall thickness. The resulting load deflection curve is shown in Fig. 7 (circles), and indicates that the imperfection simply rounds off the peak seen in the GMNA analysis, producing a slight further strength reduction ($R_{GMNIA}/R_{REF}=0.204$), together with a slightly falling postfailure curve. For a cylinder under uniform compression, an imperfection of this amplitude might have reduced the strength by 70% (Rotter 2004). This example indicates a weak imperfection sensitivity for the bracket-supported cylinder. Further studies of imperfection sensitivity, reaching the same conclusion, have been undertaken (Doerich 2007).

Interaction between Plasticity and Buckling

Although the example problem gives a good insight into the details of the behavior of this structural arrangement, it does not illustrate what changes occur as the slenderness of the system is altered, so that either buckling or plasticity might dominate. The range of possible behaviors is most easily illustrated by studying a range of geometries or material strengths that give rise to different slendernesses, using the plot proposed by Rotter (2003) to capture the full range. Here, the same shape of bracket was used, but the yield stress was modified to produce different slendernesses. This plot is shown in Fig. 13, where the ratio of the failure load of geometrically and materially nonlinear analyses to the failure load of a materially nonlinear analysis ($R_{failure}/R_{lin\ plastic}$) is plotted against the ratio of the failure load of a geometrically and materially nonlinear analyses to the failure load of a linear bifurcation analysis ($R_{failure}/R_{lin\ bif}$). High slenderness configurations are found at the bottom right, where elastic buckling at a knockdown factor of 0.67 may be seen. When the slenderness has fallen so far that $R_{failure}/R_{lin\ plastic}$ reaches 0.4, the failure begins to be noticeably affected by yielding (though local yielding has occurred in more slender cases), and plasticity begins to dominate as the stocky conditions produce failures at which the failure load of a geometrically and materially nonlinear analysis approaches the failure load of the materially nonlinear analysis (top left). For this problem, it is clear that geometric nonlinearity plays a strong role in slender structures and that elastic-plastic buckling affects a wide range of stockier geometries. The plastic collapse load is only approached for very stocky conditions. The example problem described above was chosen, with a yield stress used of $\sigma_Y=250$ MPa, to lie in the area where yielding and buckling phenomena would strongly interact.

Conclusions

This paper has presented an outline description of the behavior of a cylindrical steel shell that is discretely supported on several brackets, each of which is rigidly connected to a stiff column. The linear, materially nonlinear, geometrically nonlinear, and bifurcation behaviors of the shell have been outlined with detailed explanations of the changes in stress distribution arising from different geometrical and yield phenomena. The example shell geometry was chosen to illustrate interactions between bifurcation and plasticity in determining the failure condition. It has been shown that the behavior is not very imperfection sensitive, at least for this geometry, so design rules should not follow the corresponding formulations for uniform axial compression too closely.

The different failure behaviors of a shell of the same geometry under different analyses have been explored. In the materially nonlinear analysis, plastic collapse was achieved with membrane yield all around the bracket. By contrast, GMNA showed yielding below and beside the bracket, but compressive stresses above the bracket causing buckling. The high shear stresses on the side of the bracket did not produce buckling despite attaining the yield stress, due to their rapid decay horizontally.

This bracket problem illustrates many challenges in the interpretation of simpler computer analyses that may be used in the practical design of shells (CEN 2006). It is difficult to find a useful method of estimating of the plastic collapse strength when only linear analysis is used; the imperfection sensitivity of a system is not easily estimated on the basis of the principal stress direction causing buckling; and buckling is not easily predicted by taking the stress conditions at any single point in the structure as representing a buckling failure stress state.

References

Bijlaard, P. P. (1955). "Stresses from local loading in cylindrical pressure vessels." *Trans. ASME*, 77, 805–816.

Cai, M., Holst, J. M. F. G., and Rotter, J. M. (2002). "Buckling strength of thin cylindrical shells under localized axial compression." *Proc., 15th Engineering Mechanics Conf.*, ASCE, Reston, Va.

DASt-Richtlinie. (1980) "Beulsicherheitsnachweise für Schalen." *DASt Richtlinie 013*, Deutscher Ausschuss für Stahlbau, Köln, Germany.

Doerich, C. (2007). "Strength and stability of locally supported cylinders." Ph.D. thesis, Univ. of Edinburgh, Edinburgh, U.K.

European Committee for Standardization (CEN). (2006). "Eurocode 3: Design of steel structures, Part 1.6: Strength and stability of shell structures." *EN1993-1-6*, Brussels, Belgium.

Flügge, W. (1973). *Stresses in shells*, 2nd Ed., Springer, Berlin.

Gillie, M., Holst, J. M. F. G., Münch, M., and Rotter, J. M. (2002). "Behavior of silos supported on discrete brackets." *Int. J. Struct. Stab. Dyn.*, 2(1), 45–62.

Gould, P. L., Lowrey, R. D., Suryoutomo, H., Wang, R. S. C., and Sen, S. K. (1976). "Column supported cylindrical-conical tanks." *J. Struct. Div.*, 102(2), 429–447.

Greiner, R., and Guggenberger, W. (1998). "Buckling behavior of axially loaded steel cylinders on local supports—With and without internal pressure." *Thin-Walled Struct.*, 31, 159–167.

Guggenberger, W. (1991). "Buckling of cylindrical shells under local axial loads." *Proc., Int. Colloquium on Buckling of Shell Structures on Land, in the Sea and in the Air*, Villeurbanne, Lyon, France, 323–333.

Guggenberger, W. (1998). "Proposal for design rules of axially loaded steel cylinders on local supports." *Thin-Walled Struct.*, 31(1–3), 169–185.

Guggenberger, W., Greiner, R., and Rotter, J. M. (2000). "The behavior of locally-supported cylindrical shells: Unstiffened shells." *J. Constr.*

Steel Res., 56(2), 175–197.
Hibbit, Karlsson & Sorensen Inc. (HKS). (2003). *ABAQUS user's manual, version 6.4*, Pawntucket, R.I.
Holst, J. M. F. G., and Rotter, J. M. (2004). "Settlement beneath cylindrical shells." *Buckling of thin metal shells*, J. G. Teng and J. M. Rotter, eds., Spon, London, 129–153.
Holst, J. M. F. G., Rotter, J. M., Gillie, M., and Münch, M. (2002). Failure criteria for shells on local supports." *New approaches to structural mechanics, shells and biological structures*, H.R. Drew and S. Pellegrino, eds., Kluwer Academic, London, 315–327.
Kildegaard, A. (1969). "Bending of a cylindrical shell subjected to axial loading." *Proc., 2nd Symp. on Theory of Thin Shells*, IUTAM, Copenhagen, Springer, Berlin, 301–315.
Li, H. Y., and Rotter, J. M. (1996). "Algebraic analysis of elastic circular cylindrical shells under local loadings (Part 1 and Part 2)." *Int. Conf. on Advances in Steel Structures (ICASS '96)*, Hong Kong, 801–814 and 808814, Elsevier Ltd., Oxford, U.K.
Massonnet, C. E., and Save, M. (1972). *Plastic analysis and design of plates, shells and disks*, North-Holland Publishing Co., Amsterdam, The Netherlands.
Nemeth, M. P., and Starnes, J. H. (1998). *The NASA monographs on shell stability design recommendations—A review and suggested improvements, NASA TP 1998-206290*, Langley Research Center, Hampton, Va.
Peter, J. (1974). "Zur stabilitat von Kreiscylinderschalen unter ungleichmaessig verteilten axialen randbelastungen." Ph.D. thesis, Univ. of Hannover, Hannover, Germany.
Reissner, E. (1940). "Note on the problem of the distribution of stress in a thin stiffened elastic sheet." *Proc. Natl. Acad. Sci. U.S.A.*, 26, 300–305.
Rotter, J. M. (1998). "Shell structures: The new European standard and current research needs." *Thin-Walled Struct.*, 31(1–3), 3–23.
Rotter, J. M. (2003). "Buckling of shallow conical shell roofs for small diameter tanks and silos." *Int. Conf. on Design, Inspection, and Maintenance of Cylindrical Steel Tanks and Pipelines*, Prague, Czech Republic, 169–175.
Rotter, J. M. (2004). "Buckling of cylindrical shells under axial compression." *Buckling of thin metal shells*, J. G. Teng and J. M. Rotter, eds., Spon, London, 42–87.
Rotter, J. M., Teng, J. G., and Li, H. Y. (1991). "Buckling in thin elastic cylinders on column supports." *Proc., Int. Colloquium on Buckling of Shell Structures on Land, in the Sea and in the Air*, Villeurbanne, Lyon, France, 334–343.
Teng, J. G., and Rotter, J. M. (1990). "A study of buckling in column-supported cylinders." *Contact loading and local effects in thin-walled plated and shell structures*, V. Krupka and M. Drdacky, eds., Academia Press, Prague, Czechoslovakia, 52–61.
Teng, J. G., and Rotter, J. M. (1992). "Linear bifurcation of perfect column-supported cylinders—Support modeling and boundary conditions." *Thin-Walled Struct.*, 14(3), 241–263.
Timoshenko, S. P., and Goodier, J. N. (1970). *Theory of elasticity*, 3rd Ed., McGraw-Hill, New York.
Wang, R. S. C., and Gould, P. L. (1974). "Continuously supported cylindrical-conical tanks." *J. Struct. Div.*, 100(10), 2037–2052.
Yamaki, N. (1984). *Elastic stability of circular cylindrical shells*, Elsevier Applied Science Publishers, North Holland, Amsterdam, The Netherlands.